Thermal and Optical Properties of Gelatin/Poly(vinyl alcohol) Blends

F. H. Abd El-Kader,[1] S. A. Gafer,[2] A. F. Basha,[1] S. I. Bannan,[2] M. A. F. Basha[1]

[1]*Department of Physics, Faculty of Science, Cairo University, Giza, Egypt*
[2]*Department of Biophysics, Faculty of Science, Cairo University, Giza, Egypt*

Received 25 May 2008; accepted 7 May 2009
DOI 10.1002/app.30841
Published online 21 May 2010 in Wiley InterScience (www.interscience.wiley.com).

ABSTRACT: Differential scanning calorimetry, thermogravimetric analysis, X-ray diffraction, and ultraviolet–visible spectroscopy of gelatin and poly(vinyl alcohol) (PVA) homopolymers and their blended samples were studied. The data revealed that the gelatin and PVA polymers were compatible over the investigated range of compositions; this contributed to the formation of hydrogen-bonding interaction between their polar groups. The associated enthalpy-of-melting transition and thermal stability of the blended samples increased with increasing PVA content. This indicated that the crystalline structure of PVA was not destroyed completely in the blends, which was consistent with the X-ray diffraction pattern of the 50/50 (wt %/wt %) blended gelatin/PVA sample. The absorption edge and optical band gap for allowed direct transition were determined from ultraviolet–visible spectra. The induced changes in the band structure are elucidated. © 2010 Wiley Periodicals, Inc. J Appl Polym Sci 118: 413–420, 2010

Key words: differential scanning calorimetry (DSC); thermogravimetric analysis (TGA); UV-vis spectroscopy; X-ray

INTRODUCTION

Polymer blends are very important and belong to a rapidly advancing branch in polymer science and technology because of their widely used applications as bioequivalent materials. Gelatin is often taken as the prototype of all gel-forming systems.[1] It is derived from connective tissue protein (collagen). Poly(vinyl alcohol) (PVA) films are known to posses high tensile and impact strengths, a high tensile modulus, and excellent resistance to alkali, oil, and solvents. Additionally, PVA has gained increasing attention in the biomedical field because of its bioinertness.[2,3] A detailed literature survey suggested that little information is available on gelatin/PVA blends. Therefore, we attempted systematic studies on the structural, thermal, and optical properties of gelatin/PVA blends to better understand their compatibility and interaction.

EXPERIMENTAL

The gelatin used was a food-grade powder supplied by E. Merck (Darmstadt, Germany). Its maximum limit of ash impurity was 2.0%, and its grain size was less than 800 μm. The PVA granules were supplied by El-Nasr Co. (Cairo, Egypt). The approximate molecular weight was 125,000, the poly(vinyl acetate) residual was 0–3%, and the maximum value of ash was 0.75%.

Weighed amounts of PVA granules were dissolved in a mixture of distilled water and ethanol at a ratio of 4 : 1. Also, weighed amounts of gelatin were dissolved in distilled water at room temperature. Solutions of both PVA and gelatin were mixed together by the weight percentages 90/10, 70/30, 60/40, 50/50, and 30/70 (w/w) gelatin/PVA with a magnetic stirrer at 50°C. Thin films of these at a thickness of 0.01 cm were cast onto stainless steel Petri dishes and then dried at room temperature for about 6 days until the solvent was completely evaporated. Thermal analysis was carried out with computerized differential scanning calorimetry (DSC) and thermogravimetric analysis (TGA) instruments (TA-50) manufactured by Shimadzu Corp. (Kyoto, Japan) under an atmosphere of nitrogen at a flow rate of 30 mL/min. The heating rate used for all of the samples under investigation was 10°C/min. X-ray diffraction (XRD) patterns were obtained with XRD (Scintag) by Cu Kα radiation (Cupertino, CA), whereas ultraviolet–visible (UV–vis) spectral analysis were performed with a PerkinElmer 4-B spectrophotometer (Norwalk, CT) in the wave length range 200–900 nm.

Correspondence to: M. A. F. Basha (mafbasha@gmail.com).

The absorption coefficient (α) was determined from the UV–vis spectra with the following formula:

$$\alpha = \frac{\ln\left(\frac{1}{T}\right)}{d} \quad \text{or} \quad \alpha = \frac{A}{d} \tag{1}$$

where T is the transmittance, A is the absorbance, and d is the film thickness. The type of transitions and the value of the optical energy gap (E_g) were demonstrated by Bardeen et al.[4] as

$$\alpha h\nu = B(h\nu - E_g)^n \tag{2}$$

where $h\nu$ is the photon energy, B is a constant, and n depends on the kind of the optical transition that prevails. Specifically, the n values are 1/2, 3/2, 2, and 3 for transitions directly allowed, directly forbidden, indirectly allowed, and indirectly forbidden, respectively.

RESULTS AND DISCUSSION

Thermal analysis

The nature of the polymer blends, the water contents, and their thermal stabilities are often studied by different tools, such as DSC and TGA.

DSC

Figure 1 shows DSC thermograms of both gelatin and PVA homopolymers and blended samples with PVA contents ranging between 10 and 70 wt %. For pure gelatin during a first heating scan [Fig. 1(a), solid line], three endothermic phase transitions were seen at about 78, 214, and 313°C, and these were associated with enthalpies of 340, 32.1, and 260 J/g, respectively. The first and latter peaks were intense, whereas the intermediate peak was the minor one. The melting point of gelatin was measured with an electrothermal apparatus, and it was found to be around 312°C. Therefore, it was suggested that the endotherm observed at 313°C, in the DSC thermogram [Fig. 1(a), solid line] was due to the melting-phase transition of gelatin. The endothermic phase transition peak at 78°C may have been related to the helix–coil transition, which overlapped with the glass-transition temperature (T_g),[5–7] whereas the endothermic peak at 214°C was more uncertain, and it was probably associated with the denaturation of the gelatin segments.

In the second heating scan of pure gelatin [Fig. 1(a), dashed line], the endothermic peak at 78°C disappeared, and only a weak step baseline starting from about 58°C was exhibited, which showed the glass transition. Its characteristics were those of a completely amorphous biopolymer because of the elimination of the triple helical structure.

The DSC thermogram for pure PVA during a first heating scan [Fig. 1(b), solid line] showed two significant endothermic peaks at about 88 and 228°C, which may have corresponded to T_g and the melting-transition temperature, respectively. These values were in good agreement with those reported in the literature.[8–10] The T_g peak was broad and associated with an enthalpy of 210 J/g, whereas the melting peak associated with an enthalpy of 540 J/g was a sharp one. The broad glass transition was apparently due to the nonequilibrium structures of this process.

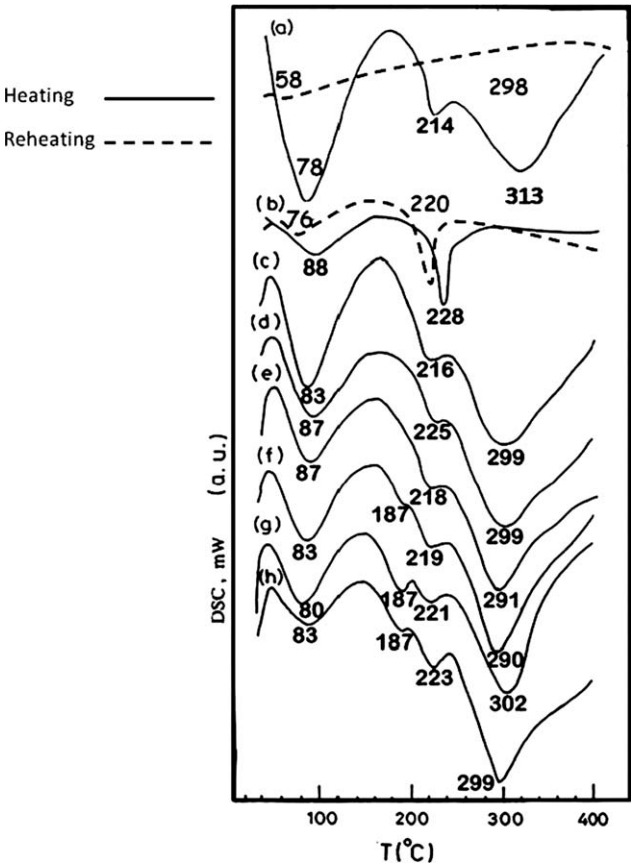

Figure 1 DSC thermograms of (a) pure gelatin, (b) pure PVA, and (c–h) 90/10, 80/20, 70/30, 60/40, 50/50, and 30/70 wt %/wt % blended gelatin/PVA samples, respectively.

The second heating scan of pure PVA [Fig. 1(b), dashed line] showed an endothermic weak glass and melting-phase transitions earlier than those reported in the first heating scan by about 20 and 15°C, respectively. Whenever the shift in the remelt was a little higher or lower than the original compound, this was probably due to oxidation of the impurities or some degradation of the polymer. The weakness and shift in the T_g value were mainly due to the evaporation of water molecules as a residual solvent.

It is of particular interest to estimate how the thermal transitions of gelatin varied with the PVA content in the blends. One key aspect was the determination of whether the resulting blended samples were compatible, that is, if they were

TABLE I
Transition Temperatures and Enthalpies Associated with Each Phase Transition for the Homopolymers and Blended Samples Measured by DSC

Gelatin/PVA (w/w)	Glass-phase transition		Melting-phase transitions				Other phase transitions			
	T_g (°C)	ΔH (J/g)	T_{m1} (°C)	ΔH (J/g)	T_{m2} (°C)	ΔH (J/g)	T_{p1} (°C)	ΔH (J/g)	T_{p2} (°C)	ΔH (J/g)
100/0	78	340	313	260	—	—	214	32.1	—	—
90/10	83	180	299	140	—	—	216	24.67	—	—
80/20	87	130	299	160	225	11.52	ND	—	—	—
70/30	87	120	291	140	218	14.64	ND	—	—	—
60/40	83	130	290	170	219	16.58	ND	—	187	4.03
50/50	80	98	302	180	221	19.13	ND	—	187	15.34
30/70	83	65.1	299	200	223	26.54	ND	—	187	10.96
0/100	88	210	—	—	228	540	—	—	—	—

T_{m2} = melting-phase transition of PVA.
ΔH, the change in the associated enthalpy; T_{m1}, melting-phase transition of gelatin; T_{p1} and T_{p2}, peak temperatures of other degradation processes.

homogeneously mixed at the molecular level.[11,12] When the polymer blend components had well-separated T_g values, an analysis of this relative to the T_g values of the component polymers could provide information about the blend phase behavior. One characteristic was that the compatible blend exhibited a single intermediate T_g between the T_g values of the pure individual polymers. Gelatin and PVA possessed T_g's that were quite close to each other, and this could cause overlapping of their individual transition peaks. Accordingly, the assessment of the transition behavior in the gelatin/PVA blends was somewhat more difficult.

The DSC thermograms of all of the blended samples [Fig. 1(c–h)] showed one single broad glass-transition peak with the maximum temperature within the range 80–87°C. However, the clearly single T_g may have been due to the difficult resolution of overlapped T_g transitions for the two blended samples. However, the position of T_g in the blended systems was found to be an intermediate of the two pure polymers, including the compatibility of the blended systems. In addition, the transition width of the T_g for the blends was almost identical to those of the pure components, which further supported single-phase behavior in the blends.

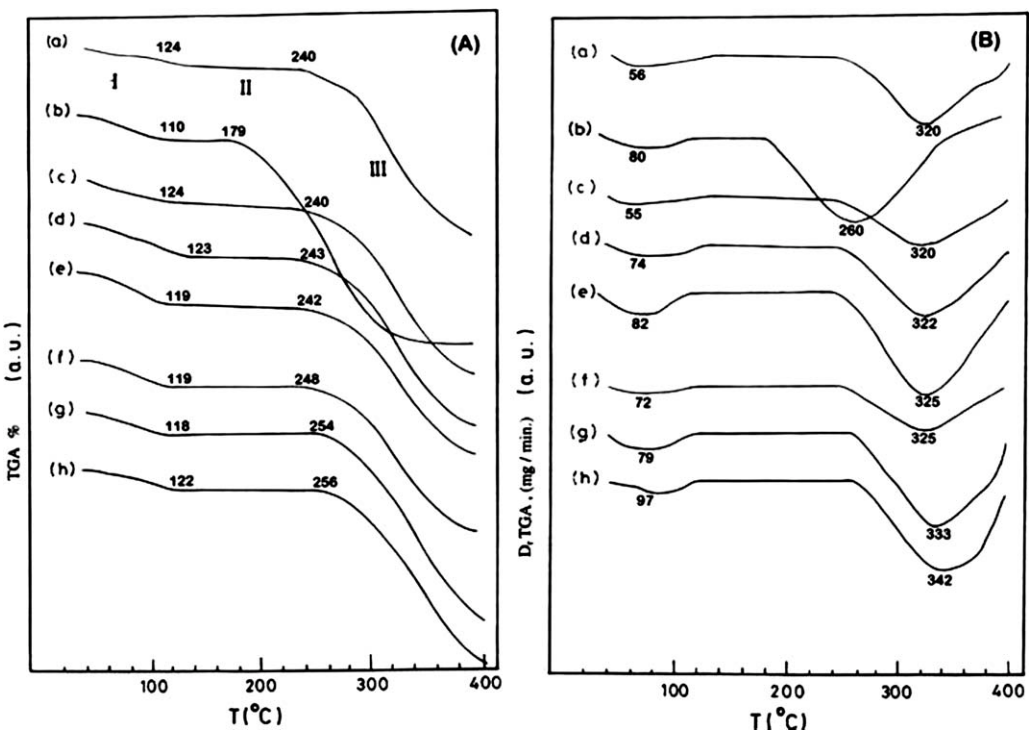

Figure 2 (A) TGA and (B) DrTGA thermograms of (a) pure gelatin, (b) pure PVA, and (c–h) 90/10, 80/20, 70/30, 60/40, 50/50, and 30/70 wt %/wt % blended gelatin/PVA samples, respectively.

TABLE II
TG and DrTG Data for the Pure Homopolymers and Blended Samples

Gelatin/ PVA (w/w)	Temperature (°C)			Weight loss (%)	
	Starting	Ending	T_p	Partial	Total
100/0	37	125	56	7.51	57.31
	240	399	320	51.90	
90/10	37	125	55	6.59	57.65
	240	400	320	50.23	
80/20	35	123	74	7.17	59.93
	243	400	322	52.76	
70/30	29	119	82	7.80	54.85
	242	399	325	46.82	
60/40	35	119	72	6.58	58.32
	248	399	325	52.18	
50/50	39	119	79	6.43	61.52
	254	398	333	54.99	
30/70	34	122	97	5.54	56.81
	256	400	342	51.51	
0/100	29	110	80	7.02	75.9
	179	398	260	67.65	

The phase-transition temperatures and the thermodynamic values associated with each transition are summarized in Table I. The melting-phase transition of PVA in the 90/10 w/w blended gelatin/PVA sample could not be detected, which may have been because of the lower percentage of PVA added to gelatin. For higher concentrations (20–70 wt %), the melting-phase transitions of PVA were observed in irregular positions with lower values of associated enthalpy compared to the pure PVA sample. The intensity and associated enthalpy of the melting-phase transition of PVA increased with increasing PVA content in the blended system (see Fig. 1 and Table I). The tendency of an apparent disproportional growth in enthalpy with the increase in the PVA content implied an increase in the degree of crystallinity in the blended samples. In addition, a new phase transition appeared at about 186 ± 1°C for the blended samples containing PVA with concentrations of 40–70 wt %. In addition, the phase transition observed at about 214 ± 1°C in pure gelatin and the 10 wt % PVA blend disappeared in the other sample.

For such blends, the differences observed in the crystallinities and phase transitions, as determined by DSC, appeared to be related to the component selection and, particularly, the relative values for the T_g's of the amorphous domains and melting transitions of the crystalline component.

Thermogravimetry (TG) and its derivative [derivative thermogravimetry (DrTG)]

The thermal degradation behavior of both the gelatin and PVA homopolymers and the blended samples were examined by TGA, as shown in Figure 2(A). All of the samples exhibited a small weight loss (5.54–7.80%, region I), beginning at about 29°C, followed by thermal stability (region II), and then by a more significant weight loss (46.82–67.66%) above 200°C for PVA and 280°C for pure gelatin and the blended samples. Table II represents the decomposition steps and percentage weight loss for individual polymers and their blends. The lower values of weight change in region I suggested that the phase transitions observed in the corresponding temperature range of the previous DSC spectra helped us the existence of a physical transition.[13] The lower values of percentage weight loss in the first decomposition step may have been due to the evaporation of water molecules or the volatilization of small molecules and/or monomers. The latter process in the TGA curves (region III) covered a wider temperature range (179.1–399.6°C), which included both melting points of individual polymers, as a physical transition, and their degradation temperatures. Therefore, the higher values of weight loss in region III indicated the existence of a chemical degradation process resulting from band scission in the polymeric backbone. This behavior may explain the increase in the values of the peak temperature (T_p)

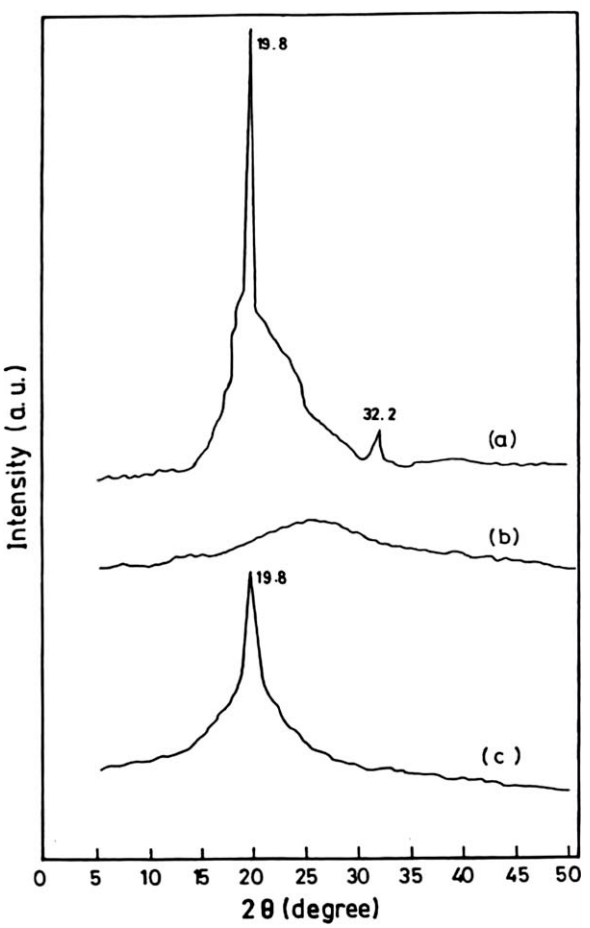

Figure 3 XRD patterns of (a) pure PVA, (b) pure gelatin, and (c) a 50/50 wt %/wt % blended gelatin/PVA sample.

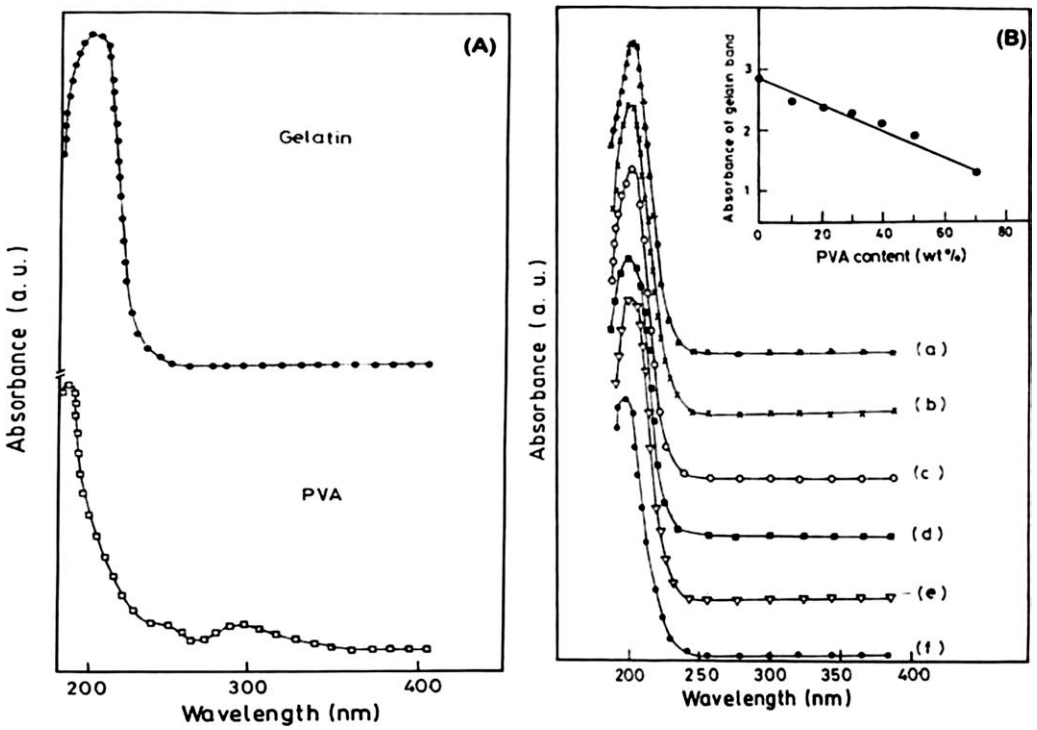

Figure 4 Absorption spectra of (A) gelatin and PVA homopolymers and (B) blended gelatin/PVA samples [(a) 90/10, (b) 80/20, (c) 70/30, (d) 60/40, (e) 50/50, and (f) 30/70 wt %/wt %].

of the derivative thermogravimetric analysis (DrTGA) obtained from TGA curves compared with the melting temperatures obtained from the DSC curves.

In addition, it is clear from Figure 2(A) that the thermal stability regions of the blended samples were higher than that of PVA, and the stabilities were enhanced by an increase in the PVA content. The difference in the thermal decomposition behavior of the different samples was shown more clearly from the DrTG curves, shown in Figure 2(B). The DrTG curves showed two broad T_p's corresponding to regions I and III. The decomposition rate of gelatin, shown as a weight loss (region III), had a maximum value at 320°C. This T_p was used as a measure of thermal stability. The relevant data are summarized in Table II.

T_p of DrTG was a function of the blended composition; it increased with increasing PVA content. Therefore, the data revealed that the thermal stability increased with increasing PVA content in the blended samples, as indicated by the shift in T_p toward higher temperature values. Thus, the higher thermal stability observed for the blended samples by TGA and its derivative were attributed to the intermolecular crosslinking reaction, which gave highly compatible impact blended polymers.[14,15]

The data obtained from DSC and TGA indicated the possibility of a strong compatibility between gelatin and PVA due to electrostatic interactions of polar —COOH— and —NH_2 groups in gelatin and —OH groups in PVA. The —OH groups were capable of hydrogen bonding. In addition, the blending compositions induced fundamental changes in the morphology of the films and their thermal stabilities.

XRD

XRD was performed to investigate whether gelatin or PVA might have been influenced by the compatibility behavior in the amorphous portion. XRD analysis[16,17] usually provides a great deal of valuable information on the configuration of macromolecules and on the structure, orientation, and size of ordered regions in the materials.

Meaningful interpretation of the experimental results required the determination of the structure of gelatin and the PVA homopolymers and the 50/50 (wt %/wt %) blended sample, that is, whether they were amorphous or crystalline. Figure 3 shows the XRD patterns of these cast film samples. Figure 3(a) shows two typical peaks for PVA, which appeared at $2\theta = 19.8$ and 32.2°.

The first reflection peak was intense and diffused in the hollow amorphous region and was assigned to a mixture of (101) and (200) planes.[18–20] The second reflection peak was weak and was assigned to the (002) plane, which agreed with that reported previously.[18–20] Figure 3(b) shows a wide

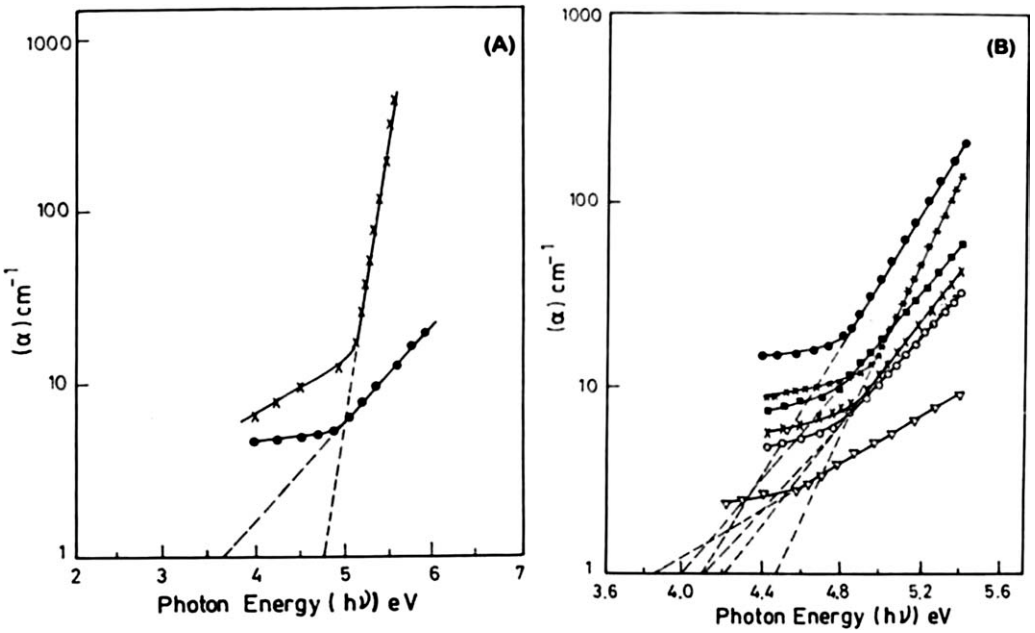

Figure 5 Variation of α with $h\nu$ for (A) homopolymers [(×) gelatin and (•) PVA] and (B) blended gelatin/PVA samples [(*) 90/10, (×) 80/20, (○) 70/30, (■) 60/40, (▽) 50/50, and (•) 30/70 wt %/wt %].

amorphous halo without any reflection, which indicated the amorphous structure of gelatin. It was reported[21] that gelatin film gave only a broad diffuse diffraction pattern typical of liquids or glassy materials, which indicated a relatively simple random coil or an amorphous structure.

The XRD pattern of the blended sample containing 50 wt % PVA exhibited the characteristics of both components [see Fig. 3(c)]. The reflection crystalline peak of PVA at $2\theta = 19.8°$ was observed with a reduction in intensity, whereas a minor reflection of PVA at $2\theta = 32.2°$ disappeared because it was masked by the amorphous halo of gelatin. Thus, we suggest that crystal forms in PVA did not prevent the compatibility between the amorphous regions of the two polymers in the blended system under investigation.

UV–vis spectra

Figure 4(A) shows the UV–vis spectra of gelatin and PVA homopolymers. The general characteristic of

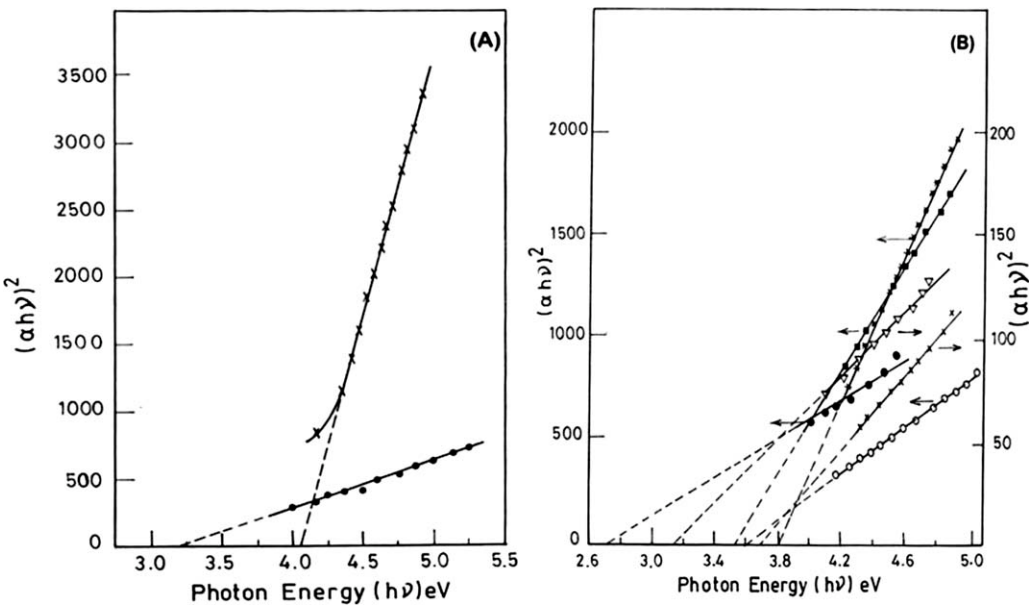

Figure 6 Plots of $(\alpha h\nu)^2$ versus $h\nu$ for (A) homopolymers [(×) gelatin and (•) PVA] and (B) blended gelatin/PVA samples [(*) 90/10, (×) 80/20, (○) 70/30, (■) 60/40, (▽) 50/50, and (•) 30/70 wt %/wt %].

TABLE III
Variations of the Absorption Edge and Allowed Direct Energy with the PVA Concentration for the Blended Gelatin/PVA Samples

Gelatin/PVA (w/w)	Absorption edge (eV)	Direct energy gap (eV)
100/0	4.79	4.07
90/100	4.47	3.83
80/20	4.21	3.69
70/30	4.1	3.66
60/40/	4.00	3.51
50/50	3.84	3.13
30/70	4.08	2.70
0/100	3.68	3.27

both spectra were that they are composed of an almost flat baseline (absorption negligible) and a steep rise near the absorption edge (remarkable absorption),.[22] The spectrum of pure gelatin film had an intense band at about 210 nm, which may have been due to the presence of chromophoric groups. This result is in good agreement with that previously reported.[23–28] In addition, the spectrum of pure PVA exhibited three absorption bands. The relatively strong band at 197 nm was associated with the presence of some residual acetate groups,[25–27] whereas the other two bands were assigned to the existence of carbonyl groups associated with the ethylene unsaturation[26,27] of the following type:

$$-(C=C)n-\underset{|}{C}=0 \qquad (3)$$

where n is 2 or 3.

Figure 4(B) shows the UV–vis spectra for the blended gelatin/PVA samples with compositions of 90/10, 70/30, 60/40, 50/50, and 30/70 (wt %/wt %) gelatin/PVA. The spectra of the blended samples contained only one sharp intense band at 210 nm for gelatin, whereas the bands of PVA disappeared. The disappearance of the absorption bands of PVA indicated that PVA became opaque in the UV region[28,29] and/or defects were induced by the mixture of the two polymers. The peak position of the gelatin band shifted toward lower wavelengths by about 10 nm with increasing PVA concentrations. In addition, the absorption intensity of the gelatin band decreased linearly with increasing PVA concentration [see the inset of Fig. 4(B)].

Figures 5 and 6 illustrate the dependence of α and $(\alpha h\nu)^2$ on $h\nu$ respectively, for the gelatin and PVA homopolymers and their blended samples. For these samples, the absorption relation $n = 1/2$, obtained by the best fit of eq. (2) applied to the curves (Fig. 6), indicated direct allowed band transition. Both the values of the absorption edge and the direct allowed band gap were determined by extrapolation of the linear portions of these curves to zero absorption. The data are presented in Table III. The values of absorption edge and direct energy gap decreased as PVA increased, reaching minimum at 50 and 70 wt %. This may reflect the induced change in the number of available final states and/or the creation of localized states in the band gap as a result of compositional disorder.[30,31] Also, the increase in the number of unsaturated defects increased the density of localized states in the band structure, which led to a decrease in the optical gap.

CONCLUSIONS

1. DSC thermograms of the blended samples showed one single broad glass-transition peak, which supported single-phase behavior in the blended systems.
2. The thermal stability of the blended samples was enhanced by increasing the PVA content, as observed in the TG curves. This was attributed to the intermolecular crosslinking reaction, which gave highly compatible impact blend polymers.
3. The XRD patterns of 50/50 (w/w) blended gelatin/PVA sample indicated that crystals formed in PVA did not prevent the compatibility between the amorphous regions of the homopolymers.
4. From the UV–vis studies, we recognized that the blend composition highly affected the polymer structure. This was clearly shown by the pronounced change in the absorption spectra and was confirmed by optical parameter data for the samples under investigation.

References

1. Rathna, G. V. N. J Appl Polym Sci 2003, 91, 1059.
2. Cholakis, C. H.; Zingg, W.; Sefton, M. V. J Biomed Mater Res 1989, 23, 417.
3. Horiike, S.; Matsuzawa, S. J Appl Polym Sci 1995, 58, 1335.
4. Bardeen, J.; Blatt, F. J.; Hall, L. H. Photoconductivity Conference; Wiley: New York, 1956; p 164.
5. Zhang, Z.; Li, G.; Shi, B. J Soc Leather Technol Chem 2006, 90, 23.
6. Mendieta-Taboada, O.; Sobral, P. J. D. A.; Carvalho, R. A.; Mônica, A.; Habitante, B. Q. Food Hydrocolloids 2008, 22, 1485.
7. Chen, C.-H.; Wang, F.-Y.; Mao, C.-F.; Liao, W.-T.; Hsieh, C.-D. Int J Biol Macromol 2008, 43, 37.
8. Alegria, A.; Goitiandia, L.; Colmenero, J. J Polym Sci Part B: Polym Phys 2000, 38, 2105.
9. Barranco, A. P.; Pinar, F. C.; Martinez, O. P. J Mater Sci Lett 2001, 20, 1439.
10. Abd El-Kader, F. H.; Gaafar, S. A.; Mahmoud, K. H.; Bannan, S. I.; Abd El-Kader, M. F. H. Curr Appl Phys 2008, 8, 78.
11. Cheuing, Y. W.; Guest, M. J. J Polym Sci Part B: Polym Phys 2000, 38, 2976.
12. Wang, H.; Hobbie, E. K.; Shimizu, K.; Wang, G. Z. G.; Kim, H. D.; Han, C. C. J Chem Phys 2002, 116, 7311.
13. Kim, J. H.; Kim, J. Y.; Lee, Y. M.; Kim, K. Y. J Appl Polym Sci 1992, 45, 1711.

14. Reich, L.; Stivala, S. S. Elements of Polymer Degradation; McGraw-Hill: New York, 1971.
15. Aggour, Y. A. Polym Degrad Stab 1996, 51, 265.
16. Tager, A. Physical Chemistry of Polymers; Mir: Moscow, 1972.
17. Cowie, J. M. G. Polymers: Chemistry and Physics of Modern Materials; Chapman & Hall: New York, 1991.
18. Tsukada, M.; Freddi, G.; Grighton, J. S. J Polym Sci Part B: Polym Phys 1994, 32, 243.
19. Cho, Y. W.; Han, S. S.; Ko, S. W. Polymer 2000, 41, 2033.
20. Nisho, Y.; Monleg, R. S. J. J Polym Sci Part B: Polym Phys 1988, 22, 1149.
21. Bradury, E.; Martin, C. Proc R Soc A 1952, 214, 183.
22. Kirschenbaum, D. M. Atlas of Protein Spectra in the Ultraviolet and Visible Regions; Plenum: New York, 1974; Vol. 2.
23. Abd El-Kader, F. H.; Osman, W. H.; Ragab, H. S.; Shehap, A. M.; Rizk, M. S.; Basha, M. A. F. J Polym Mater 2004, 21, 49.
24. Abd El-Kader, F. H.; Gaafar, S. A.; Rizk, M. S.; Kamel, N. A. J Appl Polym Sci 1999, 72, 1395.
25. Moharram, M. A.; Rabie, S. M.; El-Hamouly, W. S. J Appl Polym Sci 1991, 42, 3025.
26. Haas, H. C.; Husek, H.; Taylor, L. D. J Polym Sci Part A: Gen Pap 1963, 2, 1205.
27. Brovar, M.; Pak, V.; Kostelac Biffl, R. J Polym Sci Polym Symp 1973, 40, 19.
28. Lever, A. B. P. Inorganic Electronic Spectroscopy; Elsevier: Amsterdam, 1999.
29. Tauc, J.; Menth, A. J Non-Cryst Solids 1972, 8, 569.
30. Mott, N. F.; Davis, E. A. Electronic Processes in Noncrystalline Materials, 2nd ed.; Oxford University Press: Oxford, 1979; p 273.
31. El Samanoudy, M. M.; Ammar, A. H. Phys Status Solidi A 2001, 2, 611.